Vol 17 No 9, September 2008
1674-1056/2008/17(09)/3523-08

Chinese Physics B

© 2008 Chin. Phys. Soc.
and IOP Publishing Ltd

Phase-field study for the splitting behaviour of precipitate under applied stress*

Zhang Yu-Xiang(张玉祥), Wang Jin-Cheng(王锦程)†, Yang Yu-Juan(杨玉娟), Yang Gen-Cang(杨根仓), and Zhou Yao-He(周尧和)

State Key Laboratory of Solidification Processing, Northwestern Polytechnical University, Xi'an 710072, *China*

(Received 6 November 2007; revised manuscript received 21 November 2007)

This paper employs the phase-field method to study the splitting behaviour of a single coherent particle under an applied uniaxial stress. It finds that the splitting behaviour is greatly influenced by the initial shape of precipitates, the bulk free energy condition, the degree of supersaturation and the ratio of the interfacial energy to the elastic strain energy, etc. The simulated results demonstrate that the aspect ratio of the particle determines whether the splitting can occur and how many split plates can be obtained. The splitting of particle is sensitive to the interfacial energy, i.e. the splitting becomes more and more difficult with increasing the ratio of the interfacial energy to the elastic strain energy. And increasing the magnitude of the applied stress is favourable to the splitting. The splitting process is also explained from the point of view of the corresponding diffusion potential.

Keywords: phase-field method, splitting, precipitate
PACC: 8130H, 6400, 6470K

1. Introduction

During solid-state phase transformations, usually, the matrix and the second phase have different lattice parameters. To keep coherency in the interface region, elastic strain field often arises due to the misfit strain between the two phases. When the elastic strain field is present, the shape of a precipitate particle usually changes during growth and coarsening processes. There have been many investigations on the morphology of precipitate without the externally applied stress.[1−7] A splitting phenomenon was observed during the shape evolution experimentally which defies the conventional surface thermodynamics.[8−10] A theoretical analysis given by Khachaturyan *et al*[11] showed that a cuboidal particle will split to relax the elastic strain energy. Using microscopic diffusion theory, Wang *et al*,[3,12] also demonstrated that a single particle can split into two particles.

If an externally applied stress is present, the morphology of a coherent particle can remarkably be affected, and the splitting phenomenon can also be found. The splitting behaviour is influenced by several factors which include the magnitude of the applied stress, the degree of supersaturation, the ratio of the interfacial energy to the elastic energy, the initial shapes of particles, the interactions between particles, the misfit between phases, the type of the applied stress and the form of the incoherent bulk free energy, etc. In these previous works, some of the above factors have been analysed. Li and Chen[13] have studied the splitting behaviour of coherent particles using a diffuse-interface field kinetic method. They believed that an initially circular particle will firstly change into cuboidal shape and then split into two or more parallel plates in the subsequent evolution. Leo *et al*[14] have investigated the splitting phenomena through boundary integral method. It is demonstrated that a morphology instability driven by deviatory applied stress can generate elastically-induced particle splitting during diffusional phase transformations. However, as mentioned before, there are quite a lot of factors which can affect the splitting phenomena, and only some of them have been discussed. So, a further study is still needed to elucidate the details for the splitting of precipitate. Moreover, as to the mechanism of the splitting phenomena of precipitate under the applied stress, it is still a problem which needs further investigation. Therefore, in the present study, taking the γ/γ' system in Ni-based superalloys

*Project supported by the National Natural Science Foundation of China (Grant No 50401013).
†E-mail: jchwang@nwpu.edu.cn

as an example and using the phase-field method, we will systemically study the splitting behaviour of precipitate as well as its mechanism under an applied uniaxial stress. The effects of the shape of the precipitate, the supersaturation and the magnitude of the external stress on the spitting behaviour will be focused on.

2. Model

2.1. Phase-field model

In order to describe the kinetics of the precipitation process of the γ' phase from the supersaturated solid solution, we introduce one order parameter $c(\boldsymbol{r},t)$ to describe the composition profile, and three long-range order parameters, $\eta_1(\boldsymbol{r},t)$, $\eta_2(\boldsymbol{r},t)$ and $\eta_3(\boldsymbol{r},t)$, are needed to describe the $L1_2$ structure of the γ' phase. In this study, a single particle is investigated, these three long-range order parameters are equivalent, namely, $\eta_1(\boldsymbol{r},t)=\eta_2(\boldsymbol{r},t)=\eta_3(\boldsymbol{r},t)=\eta(\boldsymbol{r},t)$, in which $\boldsymbol{r}$ is the coordinate of the system, t the time. By solving Cahn–Hilliard equation and Ginzburg–Landau equation, the spatio-temporal evolution of the composition field and the long-range order parameter can be obtained,

$$\begin{aligned}\frac{\partial c(\boldsymbol{r},t)}{\partial t}&=M\nabla^2\frac{\delta F}{\delta c(\boldsymbol{r},t)},\\ \frac{\partial \eta(\boldsymbol{r},t)}{\partial t}&=-L\frac{\delta F}{\delta \eta(\boldsymbol{r},t)},\end{aligned}\tag{1}$$

where M is solute mobility, L the interfacial kinetic coefficient characterizing the long-range order parameter relaxation kinetics, F the total non-equilibrium free energy of the system which includes the contributions from the incoherent bulk free energy $f(c,\eta)$, the elastic strain energy, the gradient energy due to the inhomogeneities of the concentration field and the long-range order parameter. The contributions of the incoherent bulk free energy and the gradient terms can be written as,

$$F=\int_V\left(f(c,\eta)+\frac{\alpha}{2}(\nabla c)^2+\frac{3\beta}{2}(\nabla\eta)^2\right)\mathrm{d}V,\tag{2}$$

where α and β are the gradient energy coefficients. The incoherent bulk free energy can be expressed by a Landau type polynomial,[6,7,13]

$$\begin{aligned}f(c,\eta)=&\frac{1}{2}A_1(c-c_1)^2+\frac{A_2}{2}(c_2-c)\eta^2\\&+\frac{A_3}{3}\eta^3+\frac{A_4}{4}\eta^4,\end{aligned}\tag{3}$$

where A_i (i=1–4), c_1 and c_2 are phenomenological constants which can be found in Ref.[6].

2.2. Elastic strain energy equation

The elastic strain energy density of an elastically inhomogeneous system can be written as

$$f^{\mathrm{el}}(\boldsymbol{r})=\frac{1}{2}\lambda_{ijkl}(\boldsymbol{r})\varepsilon^{\mathrm{el}}_{ij}(\boldsymbol{r})\varepsilon^{\mathrm{el}}_{kl}(\boldsymbol{r}),\tag{4}$$

in which $\lambda_{ijkl}(\boldsymbol{r})$ is the elastic modulus tensor, $\varepsilon^{\mathrm{el}}_{kl}(\boldsymbol{r})$ is the elastic strain tensor which is written as,

$$\varepsilon^{\mathrm{el}}_{kl}(\boldsymbol{r})=\bar{\varepsilon}_{kl}-\varepsilon_0\delta c(\boldsymbol{r})\delta_{kl}+\frac{1}{2}\left(\frac{\partial u_k(\boldsymbol{r})}{\partial r_l}+\frac{\partial u_l(\mathbf{r})}{\partial r_k}\right),\tag{5}$$

where $\bar{\varepsilon}_{kl}$ is the homogeneous part of the total strain which is an externally applied strain if the system is under a constant strain constraint, $\delta c(\boldsymbol{r})=c(\boldsymbol{r})-c_0$, $\varepsilon_0=(1/a)(\mathrm{d}a/\mathrm{d}c)$ is the composition expansion coefficient, a is the stress-free lattice constant, c_0 is the average composition of the system, δ_{kl} is the Kronecker–Delta function, $u(\boldsymbol{r})$ is the local displacement field. The relaxation of the elastic field is much faster than the diffusion process, thus a mechanical equilibrium equation is obtained,

$$\frac{\partial\sigma^{\mathrm{el}}_{ij}(\boldsymbol{r})}{\partial r_j}=0,\tag{6}$$

by an iteration method,[15] $u(\boldsymbol{r})$ can be solved. Substituting $u(\boldsymbol{r})$ into Eq.(5), we then obtain the elastic energy density.

3. Results and discussion

In this simulation, a square domain discredited by 256×256 grid points is adopted. The semi-implicit Fourier spectral method[15] is used to solve the kinetic equations with periodic boundary conditions. The gradient energy coefficients, α=0 J/m and β=4×10^{-11} J/m, are used (the same as those in Ref.[6]). Elastic constants of the γ' and the γ phases at 1000K are $C^{\gamma'}_{11}=245$ GPa, $C^{\gamma'}_{12}=145$ GPa, $C^{\gamma'}_{44}=96$ GPa, $C^{\gamma}_{11}=202$ GPa, $C^{\gamma}_{12}=135$ GPa and $C^{\gamma}_{44}=103$ GPa, respectively.[16] To ensure that the interface contains enough mesh grids, the mesh size of 1nm is used. To guarantee the stabilization of calculation, the reduced time step used in this simulation is Δt=0.003.

3.1. Effect of the initial particle shape

In order to investigate the effect of the particle shape on the splitting behaviour, two types of particle shapes are studied, which are circular and rectangular

with different aspect ratios. In all cases, the initial matrix composition c_0 is set equal to 0.121 and $\bar{\varepsilon}_{11}$= 0.03.

3.1.1. Circular precipitate

Figure 1 shows the temporal evolution of an initially circular isolated particle of radius r=30Δx (the upper row) and the corresponding contour plots of the diffusion potential distributions (the lower row), where Δx is the dimensionless mesh size. One can see that the initially circular particle evolves towards a shape with convex faces on both the left and the right sides, and finally, it becomes a single vertical plate.

The present result is different from that of Ref.[13], which is attributed to the difference in the form of the local incoherent bulk free energy density $f(c, \eta)$. In Ref.[13], an incoherent bulk free energy density is used to provide a big difference between the equilibrium composition of matrix and precipitate, i.e., the equilibrium composition of matrix is low while that of precipitate is high. When a particle is formed in the centre of matrix with a low supersaturation, due to the high equilibrium composition of precipitate, more solute will be needed for growth, so the solute around the precipitate will easily be depleted. More importantly, due to the inhomogeneity of the diffusion potential, the solute will diffuse down the gradient of the diffusion potential, and finally, the splitting takes place. While in this study, the equilibrium composition of the matrix (c_γ=0.115) and the precipitate ($c_{\gamma'}$=0.235) cannot provide such a large gap comparing to the case of Ref.[13], and the growth cannot deplete the solute of matrix so easily. So the splitting does not occur in our study. From Fig.1(e), we can also see that the lowest value of the diffusion potential locates at the top and bottom sides of the particle. Consequently, the diffusion of solute driven by the diffusion potential gradient occurs to elongate the particle rather than splitting.

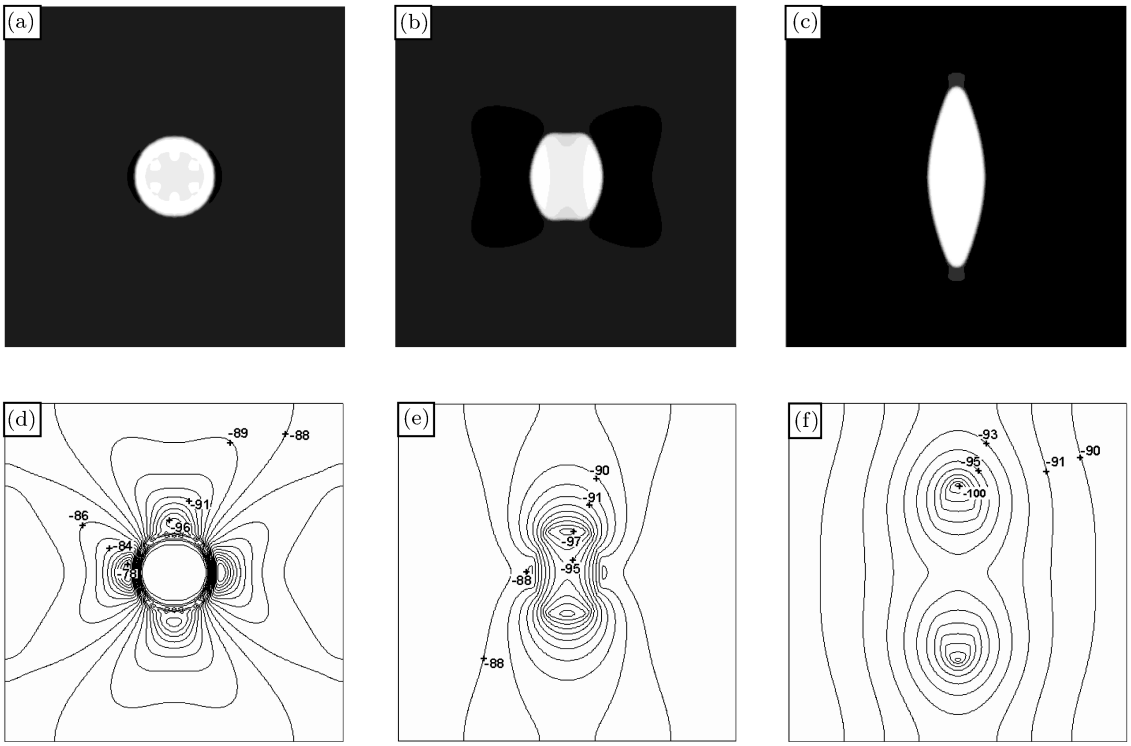


Fig.1. Evolution of an initially circular isolated particle of radius r=30Δx (the upper row) and the corresponding contour plots of the diffusion potential distributions (the lower row) with $\bar{\varepsilon}_{11}$ = 0.03. (a) t=200, (b) t=20000, (c) t=160000.

3.1.2. Rectangular precipitate

As mentioned above, the splitting phenomenon is not observed from an initially circular particle, and in the following, we will choose the rectangular shapes which will favour the splitting as the initial conditions. Three sets of rectangular particles with nearly the same initial area (for the uniform meshes are used in this study, it is difficult to get an absolutely equal

area) but different aspect ratios are selected as the initial conditions to study the splitting behaviour.

Figure 2 shows the temporal evolution of the particles with different aspect ratios of 1.0, 1.8 and 5.0 from top to bottom, respectively. The initial sizes of these three kinds of rectangular particles are $27\Delta x\times27\Delta x$, $20\Delta x\times36\Delta x$ and $12\Delta x\times60\Delta x$, respectively. As shown in Figs.2(a–c), the instability appears from the top and bottom sides of the particle and is stabilized in the subsequent evolution, the splitting cannot occur. The reason for this can similarly be found as the case of the initially circular particle. And Figs.2(d–f) show the evolution and splitting behaviour of the particle with initial size of $20\Delta x\times36\Delta x$. The instability also appears (see Fig.2(e)) and then splits the particle into two parallel vertical plates. The case with initial size of $12\Delta x\times60\Delta x$ is illustrated in Figs.2(g–i). It appears that three parallel plates vertically oriented are obtained. Comparing these results suggests that with nearly the same area as the initial conditions, the particle with high value of aspect ratio can split, but the one with a low one cannot. It is concluded that the splitting behaviour is remarkably affected by the aspect ratio of the initial particle. More plates can be obtained by increasing the aspect ratio.

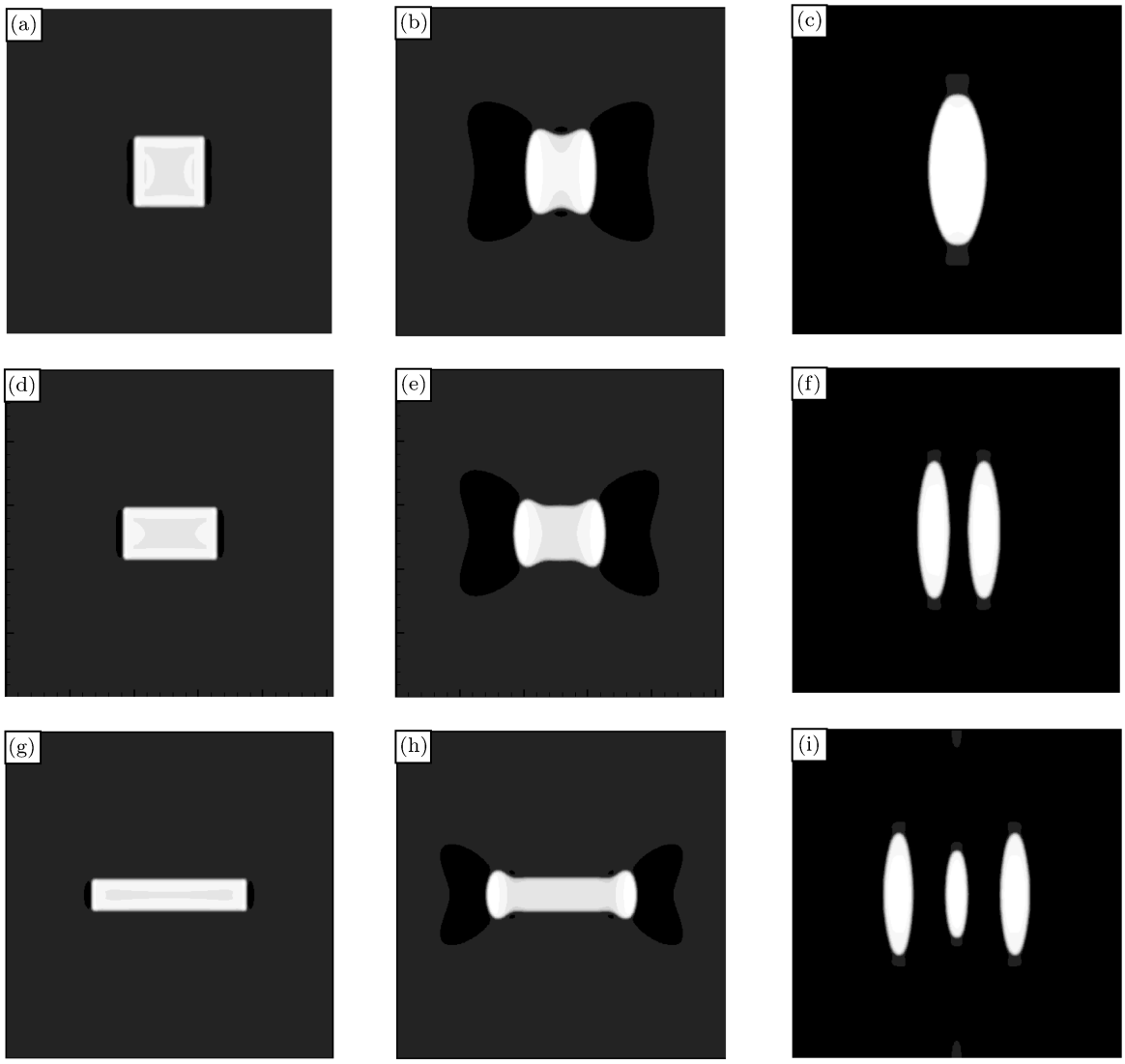


Fig.2. Evolution of an initially rectangular isolated particle (The columns from left to right correspond to t=200, 20000 and 160000, respectively.) with $\bar{\varepsilon}_{11} = 0.03$ and initial sizes of (a–c) $27\Delta x\times27\Delta x$, (d–f) $20\Delta x\times36\Delta x$, (g–i) $12\Delta x\times60\Delta x$.

As stated before, the diffusion process is determined by the gradient of diffusion potential. Figure 3 shows the nonuniform distributions of the diffusion potential for the system with initial size of $20\Delta x \times 36\Delta x$, corresponding to Figs.2(d–f), respectively. It is evident that there exists a diffusion potential gradient, which will drive the solute atoms to diffuse down this gradient. Since the elastic field is shape- and composition-dependent, the distribution of the elastic strain energy varies with the evolution process, which results in the variation of the diffusion potential distributions with time. Figure 4 shows a close-up of Fig.3(b) and indicates that the smallest value of the diffusion potential locates at the corners of the particle, which means that there exist diffusion potential gradients between the corners and the other parts around. The solute will diffuse down this gradient, i.e., the net flux of the solute is from the surrounding part to the central region of the particle. Simultaneously, there are the fluxes from the central region to the corners of the particle as shown in Fig.4 schematically by the arrow, so do the other three corners. The diffusion potential of the central region of the particle will become high with the evolution process, and it will be higher than that of the other parts inside the particle. So, there exist fluxes from the central region to the left and the right sides of the particle, and this will lead to gradual splitting.

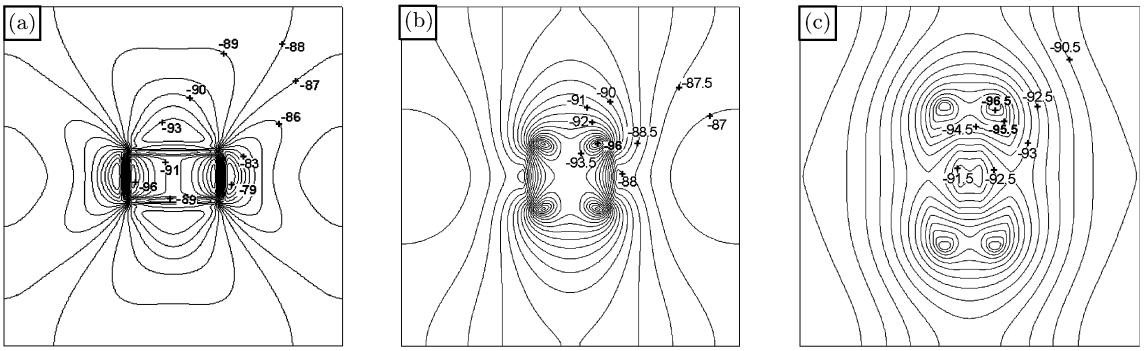


Fig.3. Contour plots of the diffusion potential distributions for the particle with initial size of $20\Delta x \times 36\Delta x$ and $\bar{\varepsilon}_{11} = 0.03$, corresponding to Fig.2(d–f), respectively. (a) t=200, (b) t=20000, (c) t=160000.

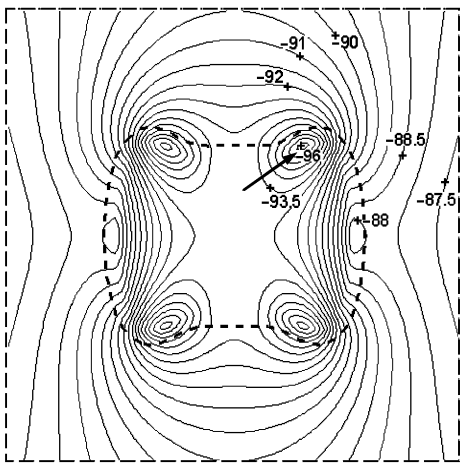


Fig.4. Contour plots of the diffusion potential distributions corresponding to Fig.3(b) (a close-up of Fig.3(e)). The dashed line denotes the contour of the particle.

Figure 5 illustrates the variations of the reduced elastic energy and the reduced interfacial energy with time for the rectangular particle with an initial size of $20\Delta x \times 36\Delta x$. It appears that the splitting is a process of increasing the interfacial energy and decreasing the elastic strain energy. The decrease of the elastic strain energy compensates for the increase of the interfacial energy, so the process can take place to lower the overall free energy of the system. From Fig.5 one can also see that the curve of the reduced interfacial energy drops sharply at the beginning, which is due to the process of diffusing the initial sharp interface.

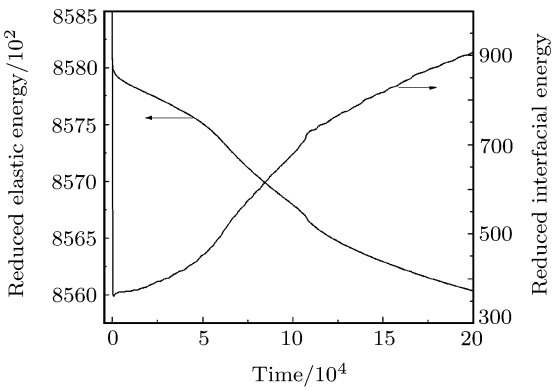


Fig.5. Variations of the reduced elastic energy and interfacial energy with reduced time for an initially rectangular isolated particle of $20\Delta x \times 36\Delta x$.

3.2. Effect of the magnitude of applied stress

To indicate the effect of the magnitude of the applied stress on splitting, we investigate the initially rectangular particle with c_0=0.121 and initial size of $20\Delta x \times 36\Delta x$. In comparison with the case of $\bar{\varepsilon}_{11} = 0.03$, in this part, $\bar{\varepsilon}_{11}$ is set equal to 0.02. The simulated results are shown in Fig.6. It is evident that the splitting cannot take place when $\bar{\varepsilon}_{11} = 0.02$ but can when $\bar{\varepsilon}_{11} = 0.03$ (see Fig.2(f)). It is obvious that the splitting of particle is quite sensitive to the magnitude of the applied stress.

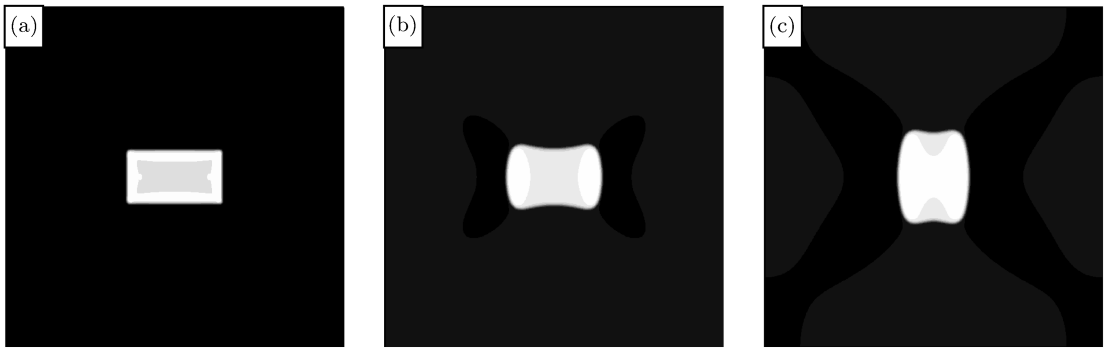


Fig.6. The evolution of an initially rectangular isolated particle with initial size of $20\Delta x \times 36\Delta x$. c_0=0.121, $\bar{\varepsilon}_{11} = 0.02$. (a) t=200, (b) t=20000, (c) t=160000.

3.3. Effect of the supersaturation

To investigate the effect of supersaturation, we study three systems. Initially, the particles are all rectangular in shape with initial size of $20\Delta x \times 36\Delta x$ and have composition of c_0=0.121, 0.13 and 0.14, respectively. And $\bar{\varepsilon}_{11}$ is 0.02 for all cases.

As shown in Fig.7, the particle of c_0=0.121 cannot split. And when c_0=0.13, although the instability appears, the splitting still cannot occur. However, the splitting can take place when c_0=0.14. It is different from the previous work which usually suggests that when the composition of matrix is low, the splitting is easier.[13] Whether the splitting can occur is determined by both the degree of supersaturation and the driving force for growth. In the system with a high degree of supersaturation, such as the case of c_0=0.14, the driving force is large and the particle has a remarkable growth process, so more solute will be needed for growth and the solute around the particle will easily be depleted. However, when the supersaturation is small, such as the case of c_0=0.121, although the amount of solute which can be depleted is small, the solute needed for growth will also be less. The particle adjusts to a vertical plate to decrease the gradient of diffusion potential (see Fig.7(a)).

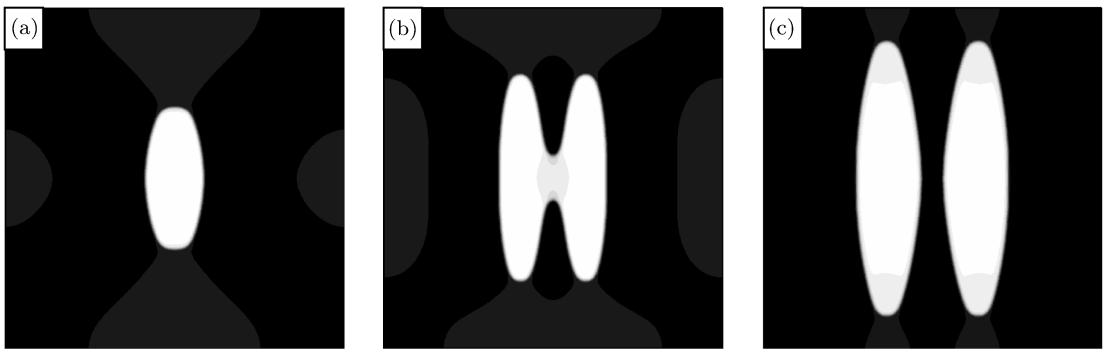


Fig.7. The morphologies of an initially rectangular isolated particle of size of $20\Delta x \times 36\Delta x$ at t=300000, $\bar{\varepsilon}_{11} = 0.02$. With alloy composition of (a) c_0=0.121, (b) c_0=0.13, (c) c_0=0.14.

3.4. Effect of interfacial energy

The splitting is a process of increasing the total interfacial energy, which is a disadvantage for the splitting of particle. As we all know, the interfacial energy can be related to the gradient coefficients α and β. In this study, we set α=0, so we can vary the value of β to change the ratio of the interfacial energy to the elastic energy. Increasing the value of β, we find that the ratio of the interfacial energy to the elastic energy is increased.

The changed β is denoted as β'. Three sets of β', β'=β, β'=2β and β'=5β, are chosen. The initial size of $20\Delta x \times 36\Delta x$ is selected. As illustrated above, at t=160000, the particle with $\beta' = \beta$ can split into two plates (Fig.8(a)). However, when β is doubled, the splitting cannot occur (Fig.8(b)) and the particle keeps single with concave interfaces on the top and the bottom sides. When $\beta' = 5\beta$, the interfacial energy is higher than that in the two previous cases. From Fig.8(c) it is seen that the splitting certainly cannot occur, it becomes one plate without any concave interface at t=160000.

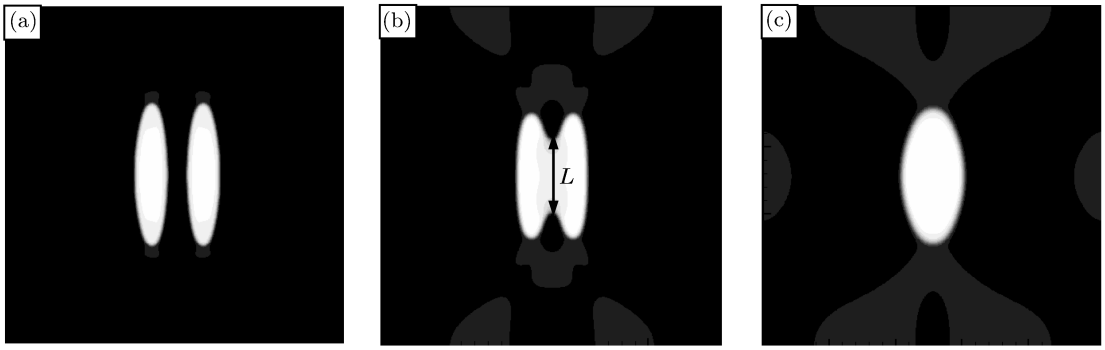


Fig.8. Morphologies of initially rectangular isolated particles with initial size of $12\Delta x \times 60\Delta x$ at t=160000, c_0=0.121. With the gradient coefficients of (a) $\beta' = \beta$, (b) $\beta' = 2\beta$, (b) $\beta' = 5\beta$.

By examining the neck distance L of the precipitate particle (as marked in Fig.8(b)), the splitting processes of particles will be known clearly. Figure 9 illustrates the evolution of L over time t for the above cases. For the case of $\beta' = \beta$, a monotone decrease of L is found in Fig.9(a). And finally, the value of L approaches zero, which corresponds to the occurrence of splitting. When $\beta' = 2\beta$, the neck distance L decreases at the early stage and then increases at later stage. As to the case of $\beta' = 5\beta$ (illustrated in Fig.9(c)), the neck distance increases over time for the whole evolution process. Therefore, it can be concluded that the splitting becomes more and more difficult with increasing the ratio of the interfacial energy to the elastic strain energy.

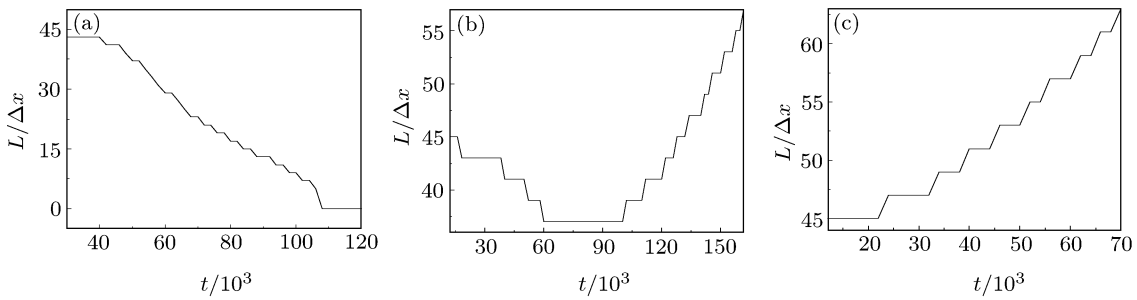


Fig.9. The neck length L as a function of time t. (a) $\beta' = \beta$, (b) $\beta' = 2\beta$, (c) $\beta' = 5\beta$.

4. Conclusions

In this study, a two-dimensional phase-field simulation was performed to investigate the splitting behaviour of a single precipitate particle under an externally applied stress. The following conclusions are obtained:

1) The splitting is ascribed to the inhomogeneity of the diffusion potential inside the precipitate particle due to the elastic strain field.

2) The splitting is greatly affected by the initial shape of the particle. In this study, an initially circular particle cannot split, while the square particles (with the same area as the circular particle) with a high value of aspect ratio can split. The higher the aspect ratio, the more plates one can obtain.

3) The splitting of particle is sensitive to the supersaturation. The splitting is determined by both the degree of supersaturation and the ability of depleting the supersaturated solute in the growth process of particles.

4) The higher the ratio of the interfacial energy to the elastic strain energy, the harder the splitting. And the larger the magnitude of the applied stress, the easier the splitting.

References

[1] Banerjee D, Banerjee R and Wang Y Z 1999 *Scr. Mater.* **41** 1023

[2] Li Y S, Chen Z, Lu Y L and Xu G D 2007 *Chin. Phys.* **16** 854

[3] Wang Y Z, Chen L Q and Khachaturyan A G 1991 *Scr. Metall. Mater.* **25** 1387

[4] Wang Y Z, Chen L Q and Khachaturyan A G 1992 *Phy. Rev.* B **46** 11194

[5] Wen Y H, Wang B, Simmons J P and Wang Y Z 2006 *Acta Mater.* **54** 2087

[6] Vaithyanathan V and Chen L Q 2002 *Acta Mater.* **50** 4061

[7] Wang Y Z, Banerjee D, Su C C and Khachaturyan A G 1998 *Acta Mater.* **46** 2983

[8] Doi M, Miyazaki T and Wakatsuki T 1984 *Mater. Sci. Eng.* **67** 247

[9] Kaufman M J, Voorhees P W, Johnson W C and Biancaniello F S 1989 *Metall. Trans.* A **20** 2171

[10] Miyazaki T, Imamura H and Kozakai T 1982 *Mater. Sci. Eng.* **54** 9

[11] Khachaturyan A G, Semenovskaya S V and Morris J W 1988 *Acta Metall.* **36** 1563

[12] Wang Y Z, Chen L Q and Khachaturyan A G 1993 *Acta Metall. Mater.* **41** 279

[13] Li D Y and Chen L Q 1998 *Acta Mater.* **47** 247

[14] Leo P H, Lowengrub J S and Nie Q 2001 *Acta Mater.* **49** 2761

[15] Hu S Y and Chen L Q 2001 *Acta Mater.* **49** 1879

[16] Wang J C, Osawa M, Yokokawa T, Harada H and Enomoto M 2007 *Comp. Mater. Sci.* **39** 871